Effect of an Oxidative Environment on the Creep Compliance of Poly(ether urethane urea)

Y. K. WU, K. R. SLETTEN, V. TOPOLKARAEV,* G. A. LODOEN, J. M. ANDERSON, E. BAER, and A. HILTNER†

Departments of Macromolecular Science and Pathology, Case Western Reserve University, Cleveland, Ohio 44106

SYNOPSIS

Secondary creep of unstabilized poly(ether urethane urea) (PEUU) in an oxidative environment appears as a linear time-dependent component superimposed on the logarithmic, viscoelastic response. The surfaces of unstabilized PEUU crept in $H_2O_2/CoCl_2$ have been characterized by scanning electron microscopy and ATR–FTIR. By examining PEUU crept for various periods of time, it is found that surface damage proceeds at gradually increasing size scales, culminating in large voids. It is hypothesized that the initial chain scission creates a flaw that grows in size under the influence of the applied load into a "nano-pit," which grows further by coalescence into a pit and, finally, a void. The initial stages of voiding occur during an induction period when there is no measurable effect on the creep response. It is possible to estimate the average compliance of the damaged PEUU by assuming a composite model with an undamaged center layer sandwiched between damaged surface layers. When the contribution of the surface layers to the creep compliance is estimated from the creep curves, the average compliance of the damaged layer is found to be about 1.6 times higher than that of the undamaged PEUU. Independent calculations of the damaged layer compliance from the void fraction indicate that the damaged layer behaves as a flexible foam in the early stages, then as a more rigid foam at longer creep times.

INTRODUCTION

Exposure of unstabilized poly(ether urethane urea) (PEUU) *in vitro* to $H_2O_2/CoCl_2$ has been used to simulate the biodegradation that is sometimes observed with long-term implantation.[1] Surface pitting and cracking on unstressed, unstabilized PEUU exposed to $H_2O_2/CoCl_2$ closely resembles the changes observed on implanted PEUU. In a previous study, effects of the oxidative environment on physical properties were evaluated in constant load creep experiments where polymer degradation was manifest as secondary creep.[2] The secondary creep response was quantitatively described by a linear time-dependent term with a characteristic induction time, superimposed on the logarithmic viscoelastic response.

Secondary creep is a well-known feature of oxidative attack on rubber vulcanizates,[3] and analytic approaches developed by Wood[4,5] and Sherby–Dorn[6] for rubber vulcanizates are adaptable to the PEUUs with modification for the induction time.[2] The influence of thickness was used to demonstrate that secondary creep in vulcanizates is a surface phenomenon.[7] It appears highly likely that secondary creep in PEUUs is also a surface effect and related to the pitting and cracking observed on unstressed PEUU.[1] It was therefore of interest to examine the surface morphology of crept PEUU and subsequently to construct a structural model that could be the basis for interpreting the creep behavior in terms of material properties of the degraded PEUU.

MATERIALS AND METHODS

The poly(ether urethane urea) (PEUU) with no added stabilizers was supplied as solution-cast films 0.18 ± 0.02 mm thick. It was prepared from MDI and poly(tetramethylene glycol) (MW = 2000) in

* On leave from the Department of Polymers and Composites, Institute of Chemical Physics, Russian Academy of Science, Moscow, Russia.

† To whom correspondence should be addressed.

Journal of Applied Polymer Science, Vol. 53, 1037–1049 (1994)
 CCC 0021-8995/94/081037-13

an approximately 1.6 to 1 capping ratio and chain-extended primarily with ethylenediamine.

Creep experiments in water, 20% H_2O_2, and 20% $H_2O_2/0.1M$ $CoCl_2$ at 37°C were carried out as described previously.[2] After creep, specimens were washed for 2 days with frequent changes of distilled water to extract excess H_2O_2 and to quench the remaining polymer free radicals. Characterization was carried out immediately.

Attenuated total reflection (ATR–FTIR) spectra were obtained on relaxed PEUU specimens using a Nicolet 800 spectrometer with a micro-ATR attachment from Harrick Scientific, Inc. The ATR–FTIR data were analyzed following procedures described previously.[8]

Specimens for scanning electron microscopy (SEM) were mounted on an SEM tensile stage and restretched to 400% elongation, then coated with 60 Å of gold and examined in a JEOL JSM-840A SEM. The micrographs were analyzed with a CUE-4 image analyzer by Olympus. Void fraction and void density were determined from analysis of several hundred voids from at least four representative areas of the micrographs.

Surface replicas of the crept specimens were prepared by casting a silicone resin, GE RTV665 with 5% GE RTV910 to reduce viscosity, on the restretched PEUU. To remove air trapped in surface pits and voids, the specimen was first coated with a thin layer of the silicone and outgassed *in vacuo* for 20 min. An additional coating of silicone made a total thickness of 1–2 mm. The silicone was cured at room temperature for 24 h. This silicone provides minimal shrinkage during curing, about 0.2%.[9] The replicas were peeled off the PEUU and viewed in the SEM at two tilting angles. The height of surface protrusions was determined by measuring the distance from the top of the protrusion to a reference point on the surface.

RESULTS

Surface Morphology

Typical creep behavior of the PEUU at 10.9 MPa is illustrated in Figure 1. Primary or physical creep was identified with a logarithmic time dependence of creep strain as seen in water and H_2O_2. When creep was performed in $H_2O_2/CoCl_2$, the onset of secondary or chemical creep at about 3600 min produced an upward deviation from logarithmic behavior. The entire creep curve was described by a modification of Wood's equation with four parameters:[2]

$$\frac{\varepsilon(t) - \varepsilon_1}{\varepsilon_1} = A \log t \qquad t < t_i \quad (1a)$$

$$\frac{\varepsilon(t) - \varepsilon_1}{\varepsilon_1} = A \log t + B(t - t_i) \qquad t \geq t_i \quad (1b)$$

where ε_1 is the instantaneous creep elongation measured at 1 min; A and B, the physical and chemical creep constants, respectively; and t_i, the induction time for secondary creep. Whereas physical creep

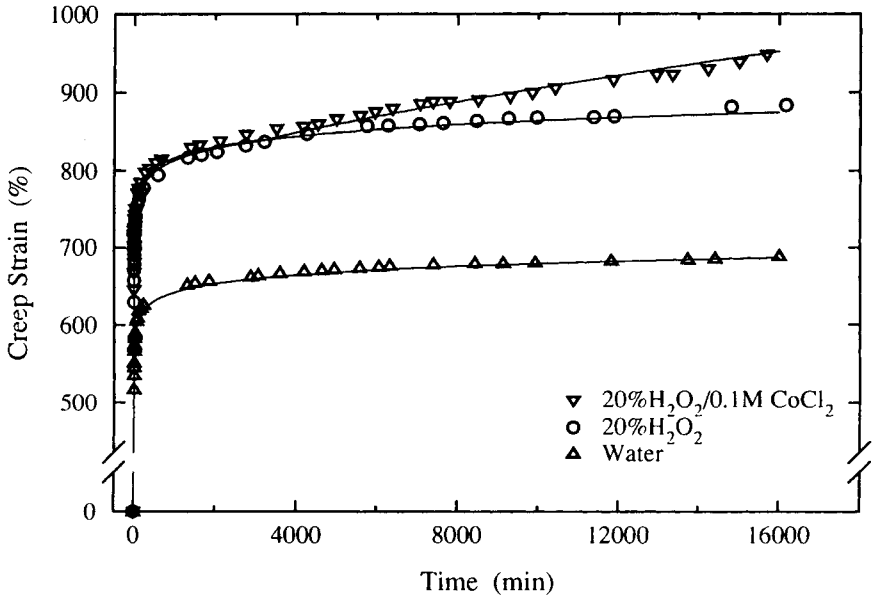

Figure 1 Creep curves of PEUU in various environments with an applied stress of 10.9 MPa. Solid lines calculated from the creep parameters and the modified Wood equation.

reflects the viscoelasticity of the PEUU, secondary creep is related to the oxidative degradation of the PEUU soft segment.

Figure 2 shows SEM micrographs of the specimens used to obtain the data in Figure 1 after termination of the creep experiment. The specimens were restretched to 400% elongation to reveal the surface morphology. The smooth, featureless surface of the specimen crept in water was indistinguishable from the untreated polymer. Small pits less than 10 μm in diameter were distributed over the surface of the specimen crept in H_2O_2, whereas numerous large voids, greater than 10 μm in diameter, covered the surface of the specimen crept in $H_2O_2/CoCl_2$. The small pits on the surface of the specimen crept in H_2O_2 had no noticeable effect on the creep behavior; however, the large voids on the $H_2O_2/CoCl_2$ specimen correlated with the appearance of secondary creep.

Specimens that had been crept in $H_2O_2/CoCl_2$ at 3.9 MPa for 16,000 min and at 12.3 MPa for 13,000 min are shown in Figures 3(a) and (b), respectively. These specimens also exhibited the large voids that appeared to be associated with secondary creep. The irregular shape of the voids suggested that they were formed by coalescence of numerous small pits. Voiding was less dense on the surface of the specimen crept at 12.3 MPa than on the one crept at 3.9 MPa. In general, with approximately the same total creep time, void density decreased as the creep stress increased. Since the initiation time for secondary creep increased with creep stress, e.g., the initiation time was 5200 min at 12.3 MPa compared to 1700 min at 3.9 MPa, the lower density of voids on the specimen crept at 12.3 MPa reflected the shorter time that this specimen had experienced secondary creep.

The time dependency of void formation is illustrated in Figure 4, where SEM micrographs of specimens crept in $H_2O_2/CoCl_2$ at 6.7 MPa for 1400, 2900, and 16,000 min are compared. Since the induction time for chemical creep at this load was 2500 min, the creep time of the specimen in Figure 4(a) was less than the induction time; in Figure 4(b), the creep time was slightly past the induction time; and in Figure 4(c), the creep time was well past the induction time. The micrograph in Figure 4(a) bears similarity to that in Figure 2(b) of the specimen crept in H_2O_2, with numerous small pits less than 10 μm in diameter distributed over the surface, although the pitting was somewhat denser on the specimen crept in $H_2O_2/CoCl_2$. When the creep time was slightly past the induction time [Fig. 4(b)], a few voids larger than 10 μm were visible where the pits had begun to coalesce, and in Figure 4(c), the large voids dominated the surface morphology.

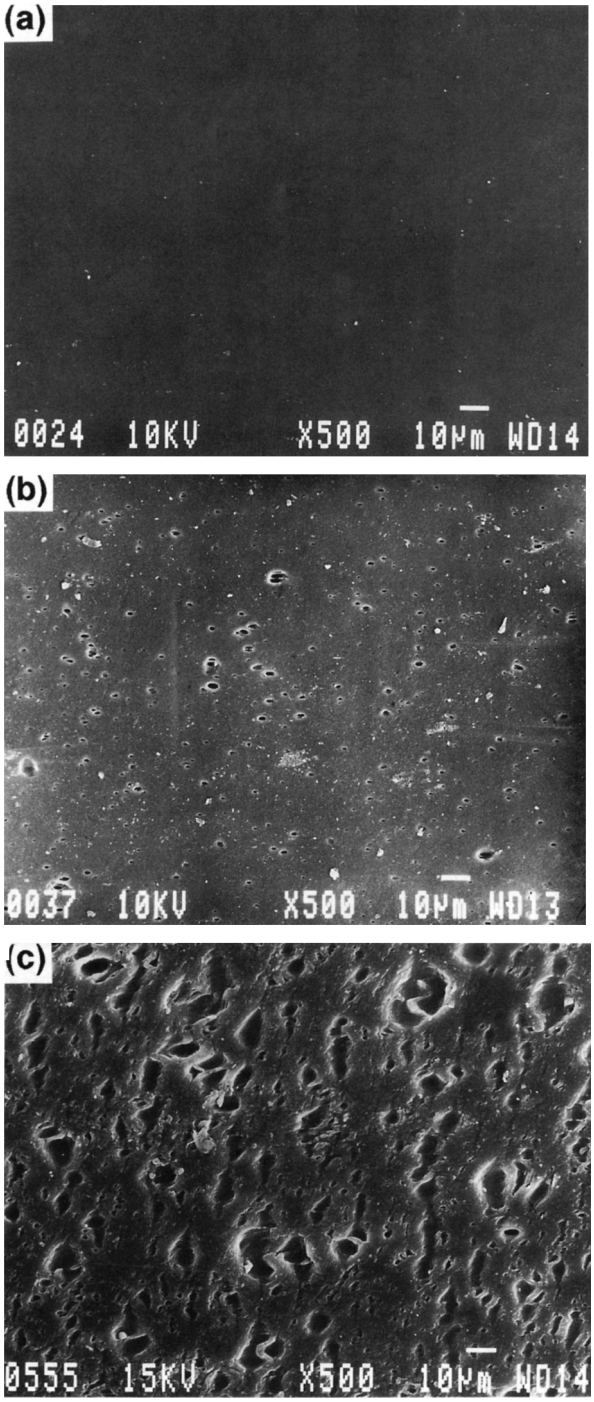

Figure 2 Scanning electron micrographs of the specimens in Figure 1 after termination of creep. Specimens were restretched to 400% elongation: (a) crept in water, (b) in H_2O_2, and (c) in $H_2O_2/CoCl_2$.

The first manifestation of chemical degradation observable in the SEM was the formation of small

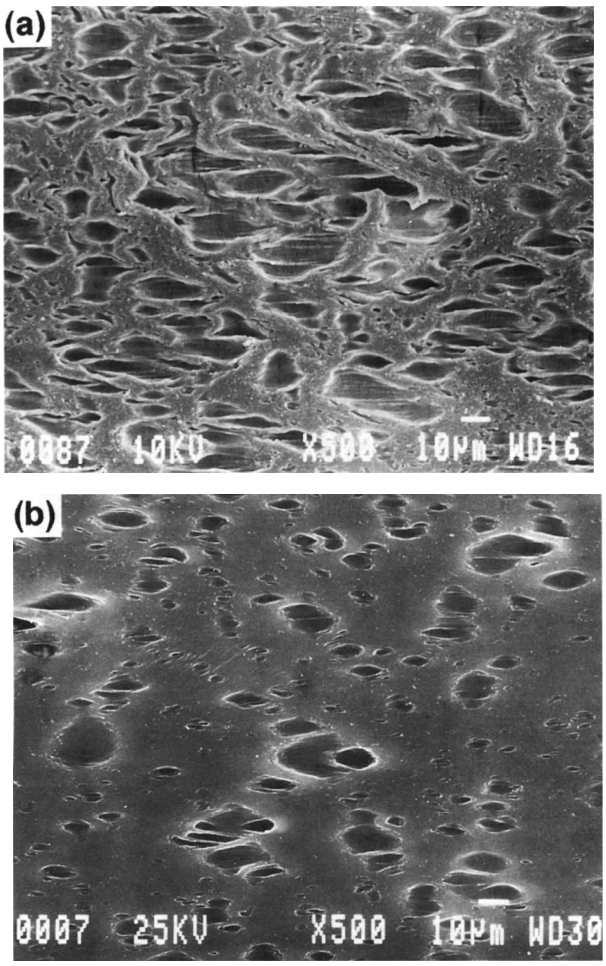

Figure 3 Scanning electron micrographs of PEUU crept in $H_2O_2/CoCl_2$ and restretched to 400% elongation: (a) crept at 3.9 MPa for 16,000 min; and (b) at 12.3 MPa for 13,000 min.

pits. These had no detectable effect on the creep behavior, presumably because they were small and isolated. The induction time for chemical creep coincided with the appearance of larger voids created by coalescence of the pits. It was hypothesized that the voided region constituted a surface layer of higher compliance that was responsible for the enhanced creep strain of specimens crept in $H_2O_2/CoCl_2$. Formation of small pits was observed with specimens crept in H_2O_2, but, presumably, these had no effect on the creep curve because they had not coalesced into voids. Without the cobaltous ion to catalyze the oxidative degradation, the reaction occurred too slowly to manifest itself in the time scale of the creep experiments; if the creep experiments in H_2O_2 had been extended to much longer times, void formation and chemical creep probably would have been observed in this environment as well.

Depth of Damaged Layer

To evaluate the depth of the voids, surface replicas were examined in the SEM at two tilt angles. Figure

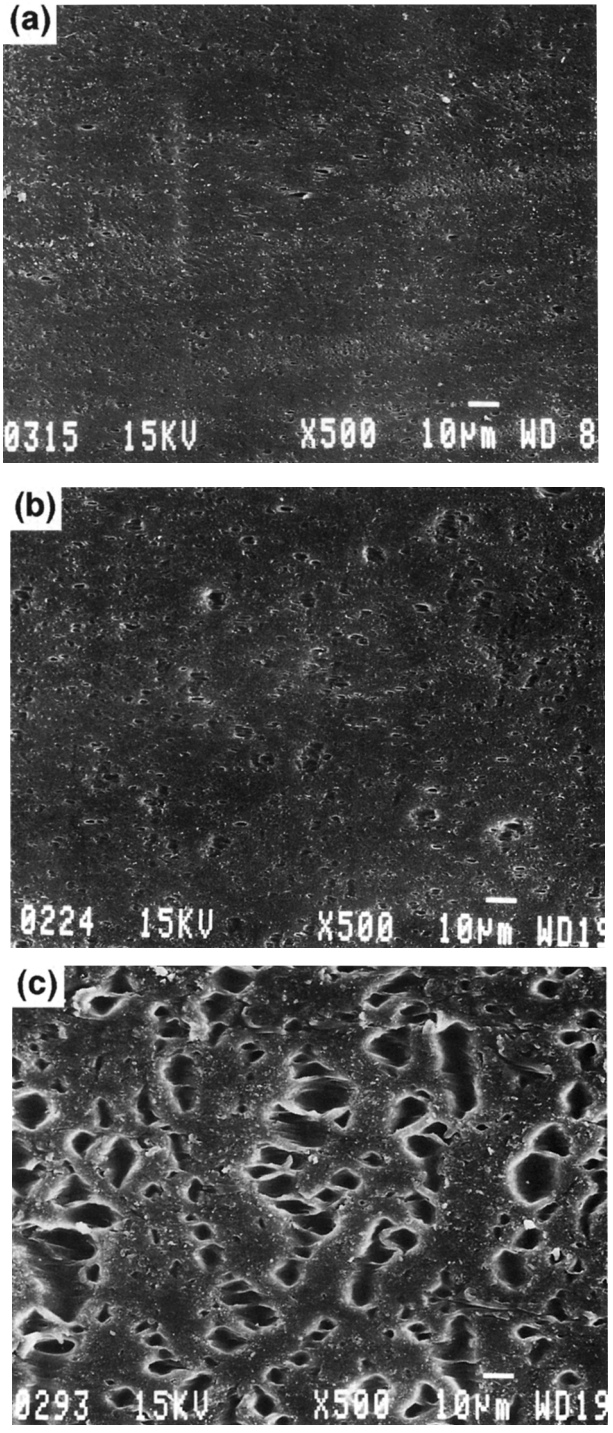

Figure 4 Scanning electron micrographs of PEUU crept in $H_2O_2/CoCl_2$ at 6.7 MPa for various periods of time and restretched to 400% elongation: (a) crept for 1400 min, (b) for 2900 min, and (c) for 16,000 min.

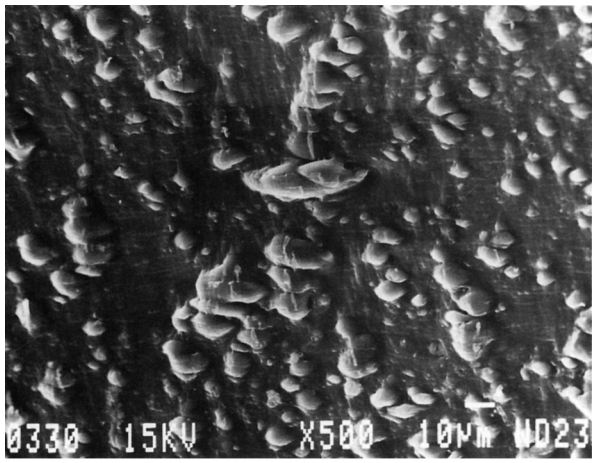

Figure 5 Silicone surface replica of PEUU crept in $H_2O_2/CoCl_2$ at 6.7 MPa for 16,000 min and restretched to 400% elongation as viewed in the SEM at a tilt angle of 30°.

5 shows a typical surface replica at a 30° tilt angle. Replication reproduced the voids as protrusions; the tops of these protrusions could be easily located and were used as the reference points for determining the height. To achieve good accuracy, higher magnification micrographs than that shown in Figure 5 were used for the analysis. In some instances, a reference point could be located at the bottom of a void, and then it was possible to use the tilting method to obtain the void depth directly from the original micrographs. The intent was to define an average depth dimension for a damaged surface layer with properties different from those of the bulk as a result of voiding. This average depth reflected the volume contribution of the voids to the damaged surface layer. Assuming that the volume was proportional to the third power of the depth (d_i), the average depth of the voided layer was defined as

$$\delta_v = \left[\frac{\sum n_i d_i^3}{\sum n_i}\right]^{1/3} \tag{2}$$

Average void depths for PEUU crept at 6.7 MPa in $H_2O_2/CoCl_2$ for various time periods are listed in Table I. The increase in δ_v was linear with time (Fig. 6), but did not extrapolate to zero time. This indicated that a period of time elapsed before pits had coalesced into voids that were large enough to measure by SEM. From the linear regression, $\delta_v = 1.53 + 0.75 \times 10^{-3}t$, and the induction time for appearance of voids obtained by extrapolation to $\delta_v = 0$ was $t_i = 2040$ min.

The existence of an induction time in void formation suggested the presence of a precursor damaged layer that contained the prevoiding phase of degradation. It was assumed that the depth of the precursor layer increased linearly with time up to the induction time and thereafter remained constant at $\delta_i = 1.53$ µm. When the depth of the precursor layer was added to that of the voided layer, the total depth of the degraded layer was given by

$$\delta_T(t) = mt \qquad t \le t_i \tag{3a}$$

$$\delta_T(t) = \delta_i + \delta_v(t) \qquad t > t_i \tag{3b}$$

This was equivalent to a vertical shift in δ_v by an amount equal to δ_i.

It appeared that the precursor layer initiated with chemical changes at the surface almost immediately after exposure of the unstabilized PEUU to the oxidative environment. One of the chemical changes known to occur in an oxidative environment is oxidative and hydrolytic chain scission at the α-methylene position of the polyol soft segment. The surface specificity of the degradation was determined from an analysis of the intensity of the 1364 cm^{-1} meth-

Table I Average Void Depth of PEUU Crept at σ_0 = 6.7 MPa

Creep Time (min)	Average Depth[a] δ_v (µm)	Total Thickness[b] d (µm)	Relative Depth[c] Δ_T
1,440	0.19	67	0.038
2,880	0.77	65	0.070
5,800	2.5	60	0.13
10,400	6.1	64	0.24
10,300	6.6	60	0.27
16,000	10.4	63	0.38

[a] From eq. (2).
[b] Restretched to 400%.
[c] $\Delta_T = 2(\delta_T/d)$.

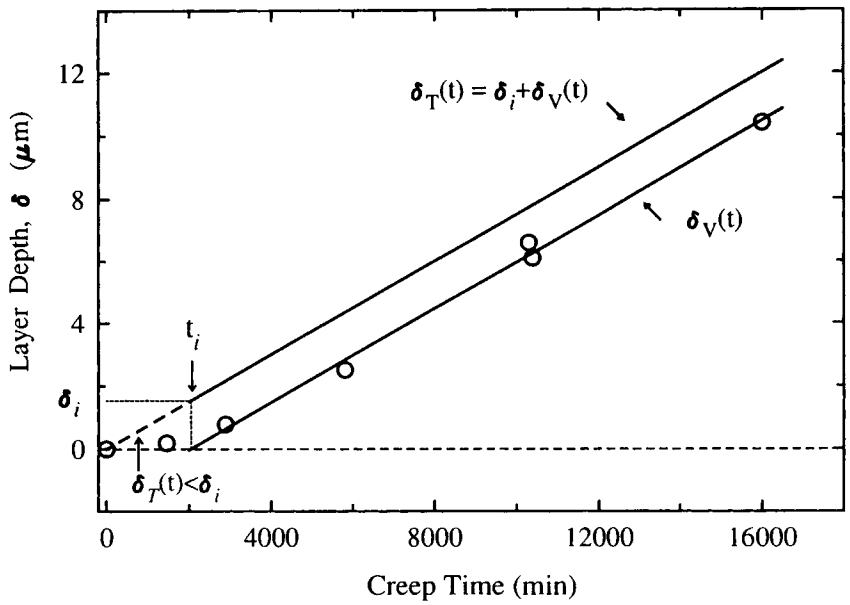

Figure 6 Depth of the damaged layer as a function of creep time in $H_2O_2/CoCl_2$ at 6.7 MPa.

ylene band in ATR–FTIR spectra obtained with different sampling depths. Following previous results,[8] it was assumed that the concentration profile could be represented by an exponential function of the form

$$C(x) = C_\infty(1 - e^{-x/h}) \tag{4}$$

where C_∞ is the bulk concentration and h is a parameter that reflects how rapidly the concentration changes in the depth direction x. The smaller h is, the more rapidly $C(x)$ approaches C_∞. The infrared absorbance A is then related to the sampling depth by

$$\left(\frac{A}{A_r}\right)^{-1} = \frac{1}{K} + \frac{2h}{K} d_p^{-1} \tag{5}$$

where A_r is the absorbance of the reference band at 1591 cm^{-1}, K is a constant that is characteristic of the primary and reference bands, and d_p reflects the sampling depth of the specific substrate. Plots of $(A/A_r)^{-1}$ as a function of d_p^{-1} were linear as shown in Figure 7 with data from specimens crept for various lengths of time in $H_2O_2/CoCl_2$. The virtually zero slope for the untreated specimen meant that the concentration of α-methylene groups was constant in the thickness direction. The plots of data from the crept specimens were also linear with the same intercept as that of the uncrept specimen. The intercept of the plot is related to K and should be the same for both crept and uncrept specimens if the concentration in the bulk does not change and degradation occurs only at the surface. From the slope of the plots, h values were obtained for the various creep times.

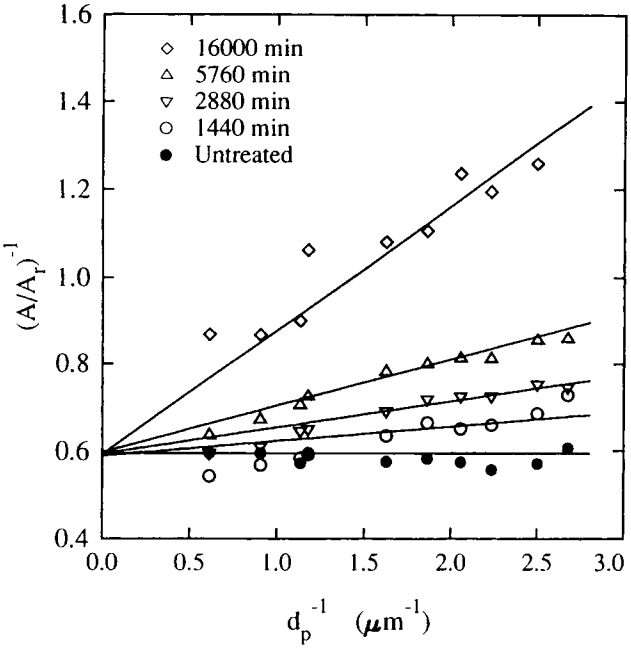

Figure 7 Relative intensity of the methylene band at 1364 cm^{-1} in ATR–FTIR spectra of PEUU crept in $H_2O_2/CoCl_2$ at 6.7 MPa for various periods of time.

Table II Depth of Chemical Degradation from Infrared Analysis

Depth (μm)	Creep Time (min)				Unstrained Implant[a]
	1440	2880	5760	16,000	
h	0.028	0.050	0.090	0.24	1.4
h_{90}	0.064	0.12	0.21	0.55	3.2
h_{99}	0.13	0.23	0.42	1.10	6.5

[a] From Ref. 8.

The data in Figure 7 and the h values in Table II were generated from the same specimens as were the SEM results in Figure 4 before they were coated with gold for SEM analysis. A change in the methylene band was detectable after the shortest creep time, which was less than the induction time for secondary creep and void formation. The magnitude of h increased approximately linearly with creep time; however, the depth of chemical degradation calculated from h and eq. (4) was much less than the depth of the voids. The depths at which the absorbance of the methylene band reached 90% (h_{90}) and 99% (h_{99}) of the absorbance in the bulk are also presented in Table II. Even after the longest creep time, the absorbance increased to 90% of the bulk absorbance within a micron of the surface. On the other hand, infrared analysis previously showed much deeper penetration of chemical degradation in unstressed, implanted PEUU (Table II). Possibly, initiation of damage sites on the surface by chemical degradation was subsequently followed by growth of pits and voids under the influence of the stress state.

DISCUSSION

Damaged Layer Compliance

Infrared analysis, and GPC molecular weight determinations reported previously,[2] showed that chem-

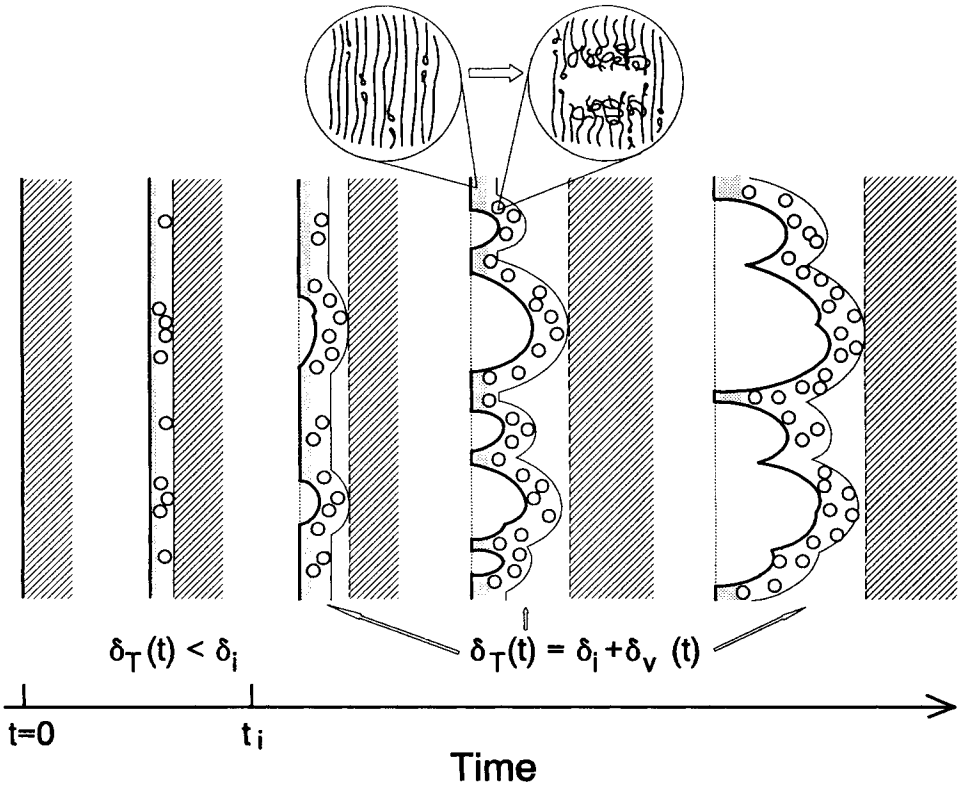

Figure 8 Hierarchy of void formation from chain scission to "nano-pit" to pit and, finally, void.

ical changes including chain scission began almost immediately after exposure of the unstabilized PEUU to the oxidative environment. Stress and strain might have affected degradation in several ways: strain-induced crystallization of the soft segments would have slowed the rate of chemical degradation; on the other hand, the applied load would have enhanced the stress concentration at weak points created by chain scission and caused them to enlarge first into small pits and then into larger voids as the pits coalesced. The chemically altered layer together with the pits constituted the precursor layer; this thin layer had no detectable effect on the macroscopic creep response.

It was speculated that degradation proceeded at gradually increasing size scales, culminating in large voids. In a hierarchical sense, illustrated in Figure 8, the initial chain scission created a flaw that grew in size under the influence of the applied load into a "nano-pit," which grew further by coalescence into a pit and, finally, a void. Depth determinations were made on the voids. The induction time for the appearance of voids (2040 min) coincided with the initiation time for secondary creep (2500 min) at the creep stress illustrated: 6.7 MPa. This suggested that the appearance of voids and the onset of secondary creep were manifestations of the same phenomenon, whereas the precursor layer did not affect the creep response of PEUU within the accuracy of the measurements. Chemical degradation only had an effect on the creep behavior when it had proceeded to the stage where voids formed.

Although the environmental changes that produce secondary creep in the PEUU are complex, involving diffusion of oxidative species and subsequent reaction with the soft segment, a simple approach for modeling the creep behavior based on a sandwich structure was attempted. In the absence of an oxidative environment, only physical creep due to the viscoelastic nature of the polymer is observed. The primary creep system in Figure 9(a) is described by the creep stress σ_p, strain $\varepsilon_p(t)$, and compliance $J_p(t)$, where the subscript p refers to the primary creep system. In an oxidative environment, the undamaged center layer is sandwiched between damaged surface layers as shown in Figure 9(b) and (c). The sandwich composite is characterized by a creep stress σ_c, strain $\varepsilon_c(t)$, and compliance $J_c(t)$. The damaged layer of the composite is the precursor layer together with the voided layer and has a higher compliance than that of the undamaged center layer. Both the thickness and compliance of the damaged

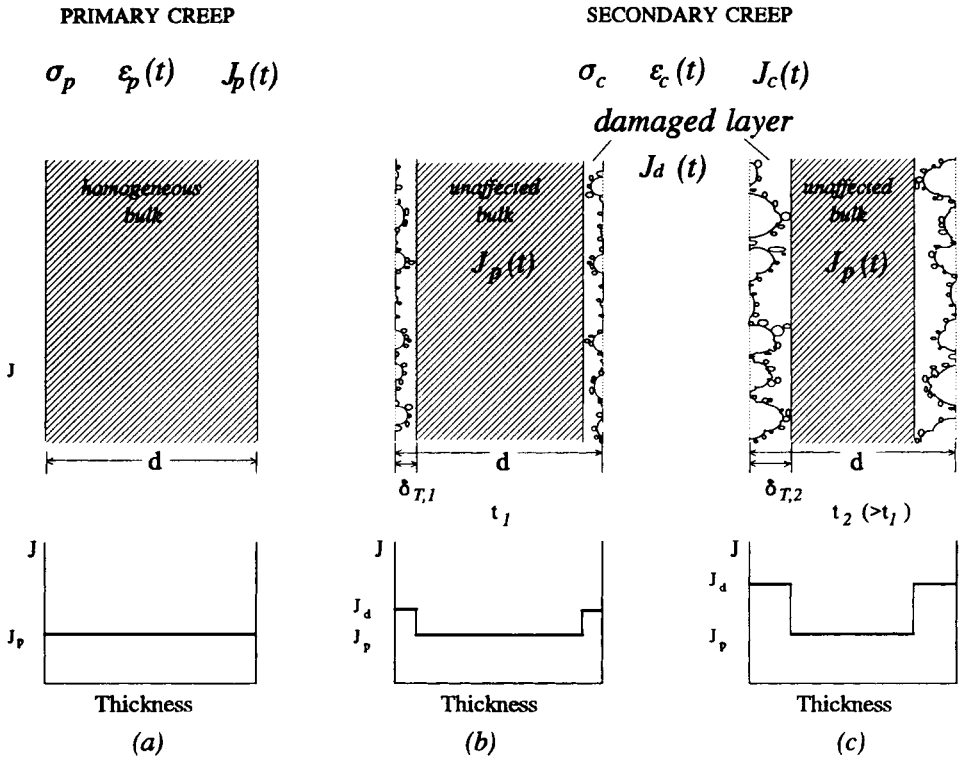

Figure 9 Sandwich model for PEUU creep: (a) primary creep system; (b) composite at t_1; (c) composite at $t_2 > t_1$.

layer increase with time. Although there is a gradient in properties through the damaged layer, for convenience, it is characterized by average values of creep stress σ_d, strain $\varepsilon_d(t)$, and compliance $J_d(t)$.

The overall compliance of the sandwich composite is higher than that of the primary creep system and also increases with time. The impact of the damaged layer on the creep curve is to cause a deviation from the logarithmic time dependency of creep strain. The contribution of the damaged surface layer to the creep compliance can be estimated from the difference between the primary (logarithmic) and composite creep curves. It is assumed that the center layer of the composite has the properties of the primary system. The creep compliance of the parallel composite model is then given by

$$\frac{1}{J_c(t)} = \frac{1 - \Delta_T(t)}{J_p(t)} + \frac{\Delta_T(t)}{J_d(t)} \tag{6}$$

where Δ_T is the fractional thickness of the damaged surface layers and is equal to $2\delta_T/d$, where d is the total specimen thickness. Because the creep strain is higher in the composite system than in the primary system at any time t, the true stress is also higher. The difference between $\varepsilon_c(t)$ and $\varepsilon_p(t)$ at any given time is in the range of 10–20%, which produces a difference in the stress of about the same amount assuming the volume of the PEUU is constant during creep. Considering the approximate nature of the modeling, this difference is small enough that for simplicity it can be assumed that $\sigma_p = \sigma_c$ at any time t. The compliance of the primary and composite systems are then related by

$$\frac{\varepsilon_p(t)}{J_p(t)} = \frac{\varepsilon_c(t)}{J_c(t)} \tag{7}$$

Combining eqs. (6) and (7), the relative compliance of the damaged layer is given by

$$\frac{J_d(t)}{J_p(t)} = \left\{1 - \frac{1}{\Delta_T(t)}\left[1 - \frac{\varepsilon_p(t)}{\varepsilon_c(t)}\right]\right\}^{-1} \tag{8}$$

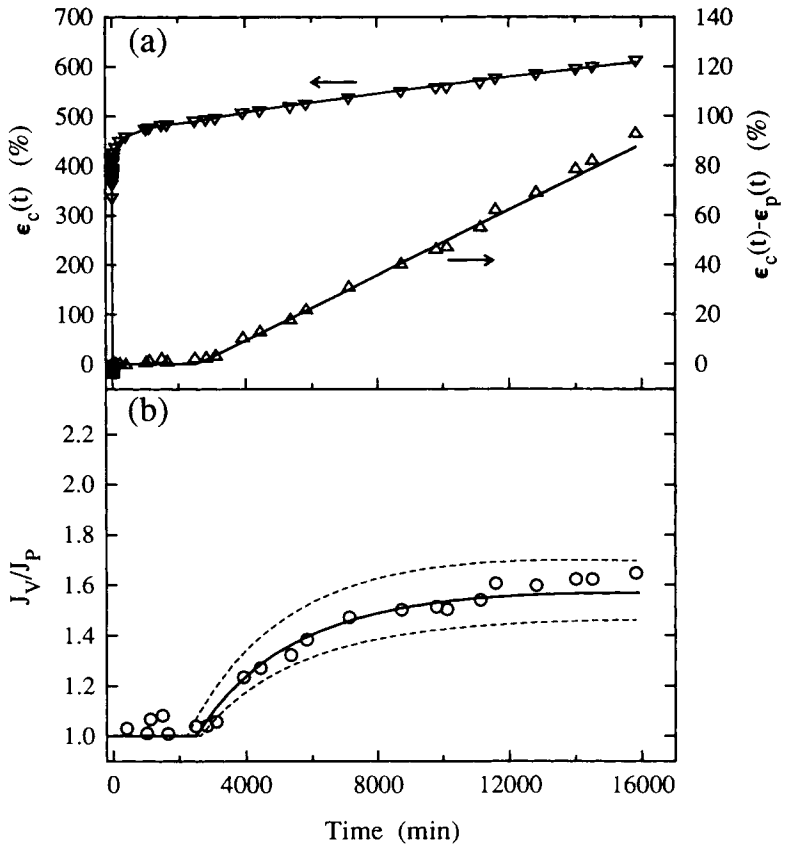

Figure 10 Creep of PEUU in $H_2O_2/CoCl_2$ at 6.7 MPa: (a) total creep strain and secondary creep strain; solid curves calculated from the creep parameters; (b) relative compliance calculated from the data points and from the creep parameters; upper and lower bounds given by dotted curves.

Table III Surface Void Fraction of PEUU Crept in $H_2O_2/CoCl_2$ at σ_0 = 6.7 MPa

Creep Time (min)	Void Fraction[a]	Void Density[a] × 10^{-6} $(cm^2)^{-1}$	Average Void Size[b] (μm^2)
2,900	0.06 ± 0.04	6.7 ± 5	0.8
5,800	0.19 ± 0.02	7.6 ± 0.6	2.5
10,300	0.22 ± 0.01	1.3 ± 0.2	17
15,800	0.32 ± 0.03	0.5 ± 0.04	60
16,000	0.31 ± 0.02	0.8 ± 0.02	37

[a] Values are mean ± standard deviation.
[b] Average void size = (void coverage)/(void density).

A typical creep curve for PEUU at 6.7 MPa in $H_2O_2/CoCl_2$ is plotted in Figure 10(a). The experimental points are indicated by open symbols, and the solid lines were calculated from empirical eqs. (1a) and (1b) using the creep parameters determined previously.[2] The upper curve represents the total creep strain of the composite system, whereas the lower solid line represents the secondary creep component alone. The experimental values of ε_c in Figure 10(a) were used with the empirical expressions for ε_p and Δ_T to calculate the relative compliance of the surface layer from eq. (8) [Fig. 10(b)]. Continuous $J_d(t)/J_p(t)$ curves were obtained by using the empirical expression for ε_c with eq. (8) and are included in Figure 10(b) for comparison. Upper and lower bounds on $J_d(t)/J_p(t)$ were determined from the standard deviation (SD) of the parameters in the creep equation (A, B, and t_i); the choice of +SD or −SD was made to give the largest deviation from the mean. The curve in Figure 10(b) shows that up to t_i, the period during which the precursor layer forms, the mean compliance of the damaged layer and the bulk are the same. With the appearance of voids at t_i, the compliance of the surface layer rapidly increases; it then gradually levels off at longer times at about 1.6 J_p as the effect of the increasing depth of the damaged layer offsets the effect of increasing void fraction at the surface.

Prediction of Damaged Layer Compliance

Several approaches were used to estimate the relative compliance of the surface layer from the void fraction. In all cases, it was assumed that the matrix material in the voided layer had the same compliance J_p as that of the primary system.

1. If it is assumed that the voids are holes through the thickness of the damaged layer with infinite compliance, the rule-of-mixtures gives the compliance of the damaged layer as

$$\frac{1}{J_d(t)} = \frac{1 - \Phi(t)}{J_p(t)} \tag{9a}$$

or the relative compliance as

$$\frac{J_d(t)}{J_p(t)} = [1 - \Phi(t)]^{-1} \tag{9b}$$

where $\Phi(t)$ is the void volume fraction of the surface layer.

2. Especially at higher void fractions, the appearance of the surface layer resembles a foam. Although various empirical approaches have been suggested for calculating the compliance of foams,[10] one that is widely used is that of Moore,[11] Throne,[12] and Pramuk[13] (M-T-P), where the rule-of-mixtures is modified with an adjustable power index to accommodate various types of foams ranging from rigid plastic foams to flexible open-cell foams. The compliance form of the M-T-P equation is

$$\frac{J_d(t)}{J_p(t)} = [1 - \Phi(t)]^{-n} \tag{10}$$

where values of n ranging from 1.4 to 1.7 have been reported for flexible foams. Since the

Table IV Relative Compliance Calculated for PEUU Crept in $H_2O_2/CoCl_2$ at σ_0 = 6.7 MPa

Creep Time (min)	Rule-of-mixtures	M-T-P	Rusch
2,900	1.1 ± 0.1	1.1 ± 0.2	1.1 ± 0.2
5,800	1.2 ± 0.1	1.4 ± 0.1	1.5 ± 0.1
10,300	1.3 ± 0.04	1.5 ± 0.1	1.7 ± 0.1
15,800	1.5 ± 0.1	1.9 ± 0.3	2.2 ± 0.4
16,000	1.5 ± 0.1	1.9 ± 0.2	2.1 ± 0.2

PEUU is very rubbery, a value of 1.7 was chosen.

3. An empirical equation has been proposed specifically for flexible open-cell polyurethane foams by Rusch.[14] The compliance is given by

$$\frac{J_d(t)}{J_p(t)} = \left\{\frac{\Psi(t)}{12}[2 + 7\Psi(t) + 3\Psi(t)^2]\right\}^{-1} \quad (11)$$

where $\Psi(t) = 1 - \Phi(t)$ is the matrix volume fraction.

To obtain the void fraction $\Phi(t)$, required in all three approaches, the surface void fraction was estimated by image analysis of the SEM micrographs and the assumption was made that the surface void fraction was equal to the volume void fraction. The void fraction for some of the specimens crept in $H_2O_2/CoCl_2$ at 6.7 MPa is given in Table III. The standard deviation was obtained by analyzing separately four areas of the micrograph, the magnitude of the standard deviation reflected the uniformity of the surface damage. The average void fraction increased continuously with creep time from about 0.19 at 5800 min to over 0.30 at 16,000 min. Furthermore, as the void fraction increased, the void density decreased due to coalescence of smaller voids into larger ones.

Values of the relative compliance of the damaged layer calculated from the three equations are listed in Table IV. In this case, upper and lower bounds on J_d/J_p were obtained from the standard deviation (SD) of the void fraction. In all cases, the rule-of-mixtures gave the lowest value, whereas the Rusch equation gave the highest value. The calculated values are compared with the curves derived from the creep parameters in Figure 11. In general, the relative compliance obtained from the creep parameters fell within the range predicted from the void fraction. At short times, when the damaged layer was relatively thin, the flexible foam models of Rusch and M-T-P fit better than does the rule-of-mixtures. At longer times, when the relative mean compliance of the damaged layer leveled off, the predicted values continued to increase. The assumption of uniform void distribution in the thickness direction was probably not appropriate for the thicker damaged layers. As the damaged layer increased in thickness, a significant gradient in the void fraction developed, with the result that the surface void fraction overestimated the volume void fraction.

A similar analysis of the relative compliance was made for PEUU crept at three stresses for about the same length of time. To obtain the relative compliance from the creep data, the depth of the damaged layer was taken as the sum of the void depth, determined from SEM micrographs, and the precursor layer depth, assumed to be independent of stress

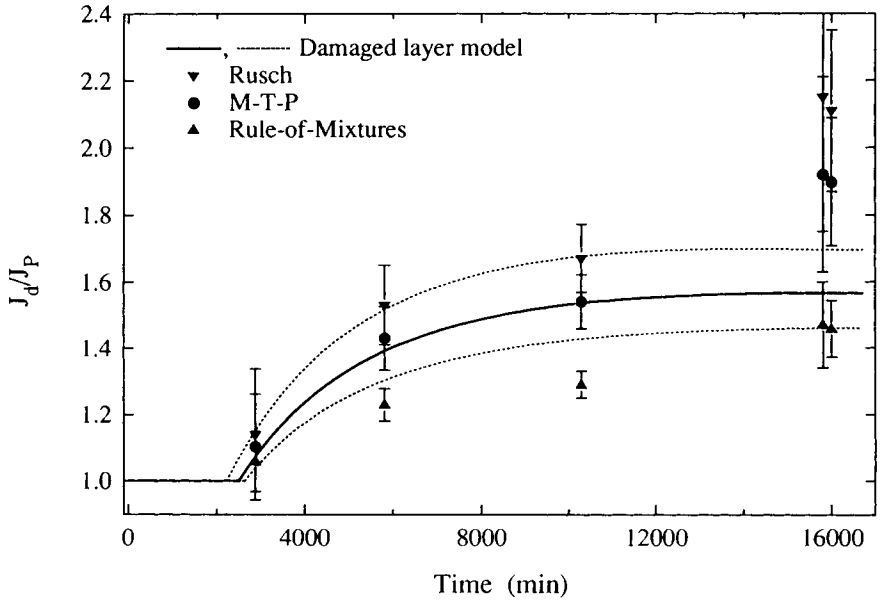

Figure 11 Relative compliance of the damaged layer calculated from creep parameters (solid lines) compared with predictions from the void fraction.

Table V Creep Parameters[a] and Surface Void Fraction for PEUU Crept in $H_2O_2/CoCl_2$

	Creep Load (MPa)		
	3.9	6.7	12.3
	Creep Time (Min)		
	16,000	16,000	13,000
ϵ_1 (%)	140 ± 3	367 ± 15	760
$A \times 10^2$	19.0 ± 0.3	11.2 ± 1.1	7.5
B (min^{-1}) $\times 10^6$	43 ± 0.9	17.4 ± 1.8	8.8
t_i (min)	1700 ± 120	2500 ± 230	5200
Void depth, δ_v (μm)	16.1	10.4	4.0
Δ_T	0.46	0.37	0.17
Average void fraction, Φ	0.55 ± 0.04	0.31 ± 0.02	0.26 ± 0.01

[a] From Ref. 2.

and equal to 1.53 μm. The surface void fraction was also determined from the micrographs. Values of these parameters, together with the creep parameters, are given in Table V. Since the initiation time for secondary creep increased with the creep stress, PEUU crept at higher stresses experienced secondary creep for a shorter period of time. This was reflected in both a smaller void depth and a lower void fraction.

The results of the relative compliance calculations using the two approaches are summarized in Table VI. The damaged layer calculation [eq. (8)] produced a relative compliance that decreased from 2.2 to 1.4 J_p as the stress increased from 3.9 to 12.3 MPa. When compared with predictions from eqs. (9b), (10), and (11), the best fit was consistently obtained with the rule-of-mixtures for these relatively long creep times. The reason that the damaged layer appeared to behave in a more rigid manner at long creep times was probably related to the gradient in the void fraction and an overestimation of the volume void fraction.

Table VI Relative Compliance, J_d/J_p, of the Damaged Surface Layer

	Creep Load (MPa)		
	3.9	6.7	12.3
	Creep Time (Min)		
	16,000	16,000	13,000
Damaged layer model	2.2 ± 0.2	1.6 ± 0.3	1.4
Rule-of-mixtures	2.2 ± 0.4	1.5 ± 0.1	1.4 ± 0.04
M-T-P	3.9 ± 1.2	1.9 ± 0.2	1.7 ± 0.1
Rusch	4.6 ± 1.5	2.1 ± 0.2	1.8 ± 0.1

CONCLUSIONS

The viscoelastic, logarithmic creep response of PEUU is modified in an oxidative environment by a superimposed linear component. This secondary creep is detectable only after a significant induction time. Examination of the surface morphology of PEUU crept in $H_2O_2/CoCl_2$ for various lengths of time reveals that the onset of secondary creep coincides with the appearance of large voids greater than 10 μm in diameter. It is hypothesized that surface damage proceeds at gradually increasing size scales, culminating in large voids. In a hierarchical sense, the initial chain scission creates a flaw that grows in size under the influence of the applied load into a "nano-pit," which grows further by coalescence into a pit and, finally, a void. The initial stages constitute an induction period and do not measurably affect the creep response.

It is possible to estimate the effect of surface damage on the PEUU compliance by assuming a composite model with an undamaged center layer sandwiched between damaged surface layers. The contribution of the damaged surface layers to the creep compliance was estimated from the creep curves; the average compliance of the damaged layer was found to be about 1.6 times higher than the undamaged PEUU. When the compliance of the damaged layer was calculated independently from the void fraction using established compliance

equations, it appeared that the damaged layer behaved as a flexible foam in the early stages, then as a more rigid foam at longer creep times.

This research was generously supported by the National Institutes of Health, Grant HL-25239.

REFERENCES

1. Q. Zhao, A. K. McNally, M. Renier, Y. Wu, V. Rose-Caprara, J. M. Anderson, A. Hiltner, P. Urbanski, and K. Stokes, *J. Biomed. Mater. Res.*, **27,** 379 (1993).
2. Y. K. Wu, G. A. Lodoen, J. M. Anderson, E. Baer, and A. Hiltner, *J. Biomed. Mater. Res.*, **28,** 515 (1994).
3. A. N. Gent, *J. Appl. Polym. Sci.*, **6,** 442 (1962).
4. L. A. Wood, G. W. Bullman, and F. L. Roth, *Rubb. Chem. Tech.*, **48,** 154 (1975).
5. L. A. Wood, *Rubb. Chem. Tech.*, **54,** 331 (1981).
6. O. D. Sherby and J. E. Dorn, *J. Mech. Phys. Solids,* **6,** 145 (1958).
7. C. Metherell, *J. Polym. Sci. Polym. Phys. Ed.*, **16,** 813 (1978).
8. Y. Wu, C. Sellitti, J. M. Anderson, A. Hiltner, G. A. Lodoen, and C. R. Payet, *J. Appl. Polym. Sci.*, **46,** 201 (1992).
9. RTV665 Data Sheet, General Electric Silicones, 260 Hudson River Rd., Waterford, NY 12188, February, 1992.
10. N. C. Hilyard and J. Young, in *Mechanics of Cellular Plastics,* N. C. Hilyard, Ed., Applied Science, London, 1982, Chapt. 1, pp. 1–26.
11. D. R. Moore, K. H. Couzens, and M. J. Iremonger, *J. Cell. Plast.*, **May/June,** 135 (1974).
12. J. L. Throne, *J. Cell. Plast.*, **Jan/Feb,** 21 (1978).
13. P. F. Pramuk, *Polym. Eng. Sci.*, **16,** 559 (1976).
14. K. C. Rusch, *J. Appl. Polym. Sci.*, **13,** 2297 (1969).

Received January 11, 1994
Accepted February 25, 1994